Nano World Journal

https://doi.org/10.17756/nwj.2023-s2-067

Research Article

Open Access

Adsorption of Organic Pollutants Using Moroccan Oil Shales: Optimization of the Adsorption Process Using a Factorial Design

Anas Krime[1*], Sanaâ Saoiabi[1], Soumia Berrahou[1], Souhayla Latifi[1,2], Larbi El Hammari[1] and Ahmed Saoiabi[1]

[1]Laboratoire de Chimie Appliquée des Matériaux, Department of Chemistry, Faculty of Sciences, Mohammed V University in Rabat, Morocco

[2]Laboratory REMTEX, ESITH (Higher school of textile and clothing industries), Casablanca, Morocco

[*]Correspondence to:
Anas Krime
Laboratoire de Chimie Appliquée des Matériaux, Department of Chemistry, Faculty of Sciences, Mohammed V University in Rabat, Morocco.
E-mail: anas.krime@um5r.ac.ma

Received: July 25, 2023
Accepted: September 26, 2023
Published: September 29, 2023

Citation: Krime A, Saoiabi S, Berrahou S, Latifi S, El Hammari L, et al. 2023. Adsorption of Organic Pollutants Using Moroccan Oil Shales: Optimization of the Adsorption Process Using a Factorial Design. *NanoWorld J* 9(S2): S396-S400.

Published by United Scientific Group

Abstract

There is currently worldwide interest in the use of inexpensive, naturally available adsorbent materials for contaminant removal. In our research work, the oil shale of the Moroccan Rif region has been used as an adsorbent for ciprofloxacin (CIP) adsorption studies in an aqueous solution. Raw oil shale has been characterized by different analysis techniques to study its structural and textural properties. The results of the characterizations by X-ray diffraction (XRD), Fourier-transform infrared spectroscopy (FTIR), and thermogravimetric analysis (TGA) showed that the OST100 has a SiO_2 (Silicon dioxide)-quartz phase which is very interesting for the adsorption of organic species (Antibiotic). Design-Expert software was used to examine the influence of different organic pollutants concentrations, oil shale mass, and contact time on organic pollutants removal efficiency using oil shales. Additionally, the correlation between the actual and theoretical removal efficiencies of toxic antibiotics was analyzed, assessing the degree to which the predicted distribution results aligned with the experimental values.

Keywords

Water pollution, Moroccan oil shales, Adsorption, Optimization

Introduction

Environmental contamination produced by the increase in population size and human activities has become a major problem in all countries of the world and therefore can pose a threat to human health and eco-environmental security [1]. Water quality has been influenced by many factors such as rainfall, geology, climate, urban development, agriculture, vegetation, soil, flow conditions, groundwater, and human activities [2]. The biggest threat to water quality is from industrial point sources, the most common contaminants of which are drugs [3].

Pharmaceutical antibiotics are widely used in veterinary and human medicine, natural chemical substances produced by microorganisms that constitute an important group of new pollutants [4, 5]. Special attention is given to antibiotics because they can inhibit the growth or destroy certain bacteria or other microorganisms even in relatively low concentrations [6-8]. In addition, their inefficient biodegradation in nature, including surface, groundwater, and domestic water, threatens the ecosystem and human health [9]. Antibiotic, CIP, a typical second-generation quinolone or fluoroquinolone family antibiotic, is one of the most rejected antibiotics found in water and wastewater [10]. However, like other antibiotics, CIP can pose a serious health risk [11, 12] and predict severe toxicity to aquatic plants and animals. Therefore, effective removal of CIP is plausible due to their high concentration in drain waters, and their resistance to degradation [13].

Up to the present time, a lot of methods have been investigated to eliminate CIP from aqueous solutions, including chemical oxidation [14], membrane filtration [15], biodegradation [16], ion exchange [17], ultrafiltration [18], reverse osmosis [19], electrocoagulation [20], and adsorption [21]. Most of these methods have some disadvantages, such as high operation and maintenance costs and the use of toxic chemicals [22], which severely limit their widespread use. Adsorption, which is one of the most favorable methods for the treatment of antibiotic-rich wastewater, was studied on account of its cost-effective, simple, and effective characteristics.

Adsorption is a powerful and easy-to-enforce approach for the removal of certain organic pollutants (Antibiotics). However, its effectiveness relies upon lots on the character of the assist used as an adsorbent, especially regarding its cost, its availability, and its regeneration [23]. Within this framework, oil shale-based materials have garnered considerable interest as cost-effective and easily accessible adsorbents. Notably, Morocco stands as the sixth-largest holder of substantial oil shale reserves globally, following the United States. Therefore, the oil shale of the Moroccan Rif region is a good adsorbent of organic and inorganic pollutants, because of having SiO_2 as the main phase [24].

In this work, the raw oil shales had been used as an adsorbent of CIP discovered in wastewater, and to lessen the wide variety of experiments, time, and average system cost, a technique factorial design was used. This technique is also used to develop adsorption in various applications and obtain a better response.

Materials and Method

Materials

As mentioned in our previously reported method, the oil shale used in the adsorption process originates from the Rif deposit in northern Morocco [25]. Recall that the shale sample was crushed, sieved into the 100 - 500 µm particle size fraction, and washed several times with water. The Moroccan oil shale was then steamed at 100 °C and designated as OST100. All used materials are nanoscale materials.

Characterization of oil shales

To determine the atomic arrangement of the crystallized structure and identify the nature of the phases present in OST100, XRD was performed using an Advance diffractometer (Bruker D8, Cu-κα radiation). The molecular structures and chemical bonds of oil shale were studied using an FTIR, and TGA of OST100 was performed at a heating rate of 5 °C/min under air (At a temperature range of 25 °C to 800 °C). The porous and external surface of OST100 was calculated by adsorption of nitrogen gas (BELSORP-max, 77 K) and applying the BET (Brunauer-Emmett-Teller) equation.

Preparation of CIP solution

A Commercially prepared CIP solution with a molar mass of 331,346 g/mol. The dilution in distilled water was carried out from the stock solution to obtain different concentrations of ciprofloxacin from 5 ppm to 100 ppm. The investigated amount of CIP adsorbed on oil shale was obtained by UV-Visible spectroscopy (UV-3100PC).

Adsorption experiment

Adsorption tests were controlled to evaluate the efficiency of crude and calcined oil shale when 0.2 g of adsorbent was exposed to 100 ml of the desired drug solution (At a temperature of 25 °C). After stirring this mixture for six hours, the CIP content was determined using a UV-Visible spectrophotometer (λ_{max} = 275 nm). The following equation was used to calculate the amount of antibiotic absorbed at equilibrium (R).

$$R = \frac{(C_0 - C_e)}{m} V$$

Where C_0 and C_e are CIP's initial and equilibrium concentrations (ppm), respectively. V is the volume (L) of the antibiotic solution, and m is the weight (g) of the sorbent.

Design and optimization

To investigate the effect of experimental factors (OST100 mass, initial concentrations, and stirring time) on CIP adsorption, Design-Expert 11 software was employed [26]. All experiments were performed corresponding to a design matrix based on the number of studied variables. Each variable has three levels, coded -1 for the low level, 0 for the medium level, and +1 for the high level (Table 1). The matrix used in this study consisted of 15 passages (Table 1) [27].

Table 1: Different levels for Design-Expert 11 software.

Factors	Symbol	Levels	
		-1	+1
Mass (g)	A	0.1	0.4
Initial concentration (mg/L)	B	10	100
Contact Time (min)	C	1	360

Results and Discussion

XRD analysis

Diffraction patterns of oil shale (OST 100) show small peaks at low intensity at 2θ = 29.2°, 34.8° and 61.8° corresponding (Based on chemical analysis) to $CaCO_3$, Fe_2O_3, and Al_2O_3 [28]. In addition, intense peaks are indicative of primarily SiO_2 quartz (Figure 1). Crystal parameters, cell type, space groups, and volume are presented in table 3.

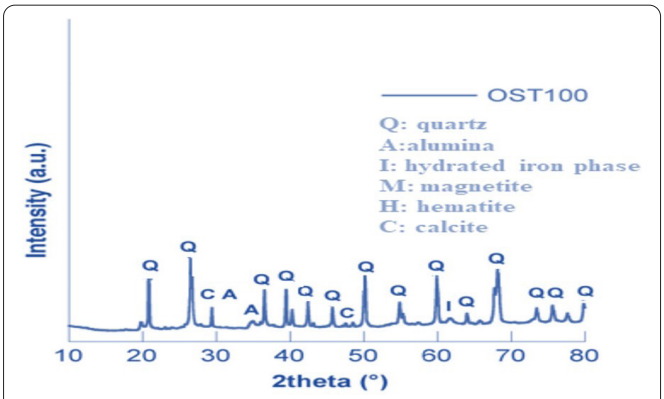

Figure 1: XRD diffractograms of OST100.

Table 2: The design matrix used in this study.

Run	Factor 1: A (g)	Factor 2: B (mg/g)	Factor 3: C (Min)	Response: R (mg/g)
1	0.256	55	167.935	19.56
2	0.256	55	167.935	19.56
3	0.256	10	360	18.92
4	0.211	59.95	1	12.57
5	0.211	10	203.835	9.2
6	0.211	100	360	37.5
7	0.1	10	1	7.6
8	0.1	100	132.035	26.55
9	0.1	43.75	360	13.58
10	0.286	100	1	6.8
11	0.286	45.1	184.09	23.28
12	0.286	100	360	37.5
13	0.4	100	149.985	22.18
14	0.4	41.5	360	29.84
15	0.4	10	1	6.93

Table 3: Symmetry properties of OST100 and their representations.

	Fe_2O_3	SiO_2	Al_2O_3
Space group	R3C	P321	Fd3m
Mesh type	Rhombohedral	Compact hexagonal	Cubic face centered
Crystalline parameters	a = b = 5.0356 Å c = 13.07489 Å	a = b = 4.9139 Å c = 5.4057 Å	a = b = c = 7.914 Å
Mesh Volume	301.326 Å3	47.9641 Å3	495.66 Å3

FTIR analysis

Oil shales studied have two absorption bands characteristic of hydroxyl ions in the IR spectrum at approximately 3560 cm^{-1} and 630 cm^{-1}, which means that the studied oil shale is hydroxylated [28]. FTIR spectra also show peaks at 3380 cm^{-1}, 2280 cm^{-1}, 2170 cm^{-1}, and 1969 cm^{-1} due to the presence of trace amounts of carbonyl compounds. In addition, figure 2 presents several bands especially those due to SiO_2 groups, Si-O groups of symmetric, asymmetric, and strain absorption bands between 1158 cm^{-1} and 400 cm^{-1}.

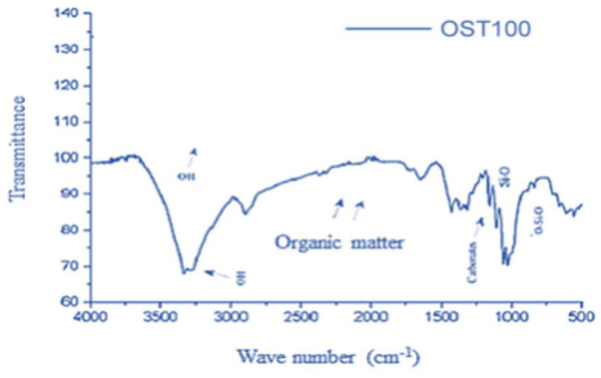

Figure 2: FTIR spectra of raw oil shale.

TGA and BET analysis of OST100

BAs shown in figure 3, a gradual weight loss corresponding to 1 wt.% of the starting material was observed after the desorption of weakly bound water between 200 and 700 °C due to the decomposition of organic matter.

Figure 3 also shows that the specific surface area of OST100 is on the order of 23 m^2/g [28] and this confirms that our oil shale is type IV (Mesoporosity) according to the characteristic Brunauer classification [29].

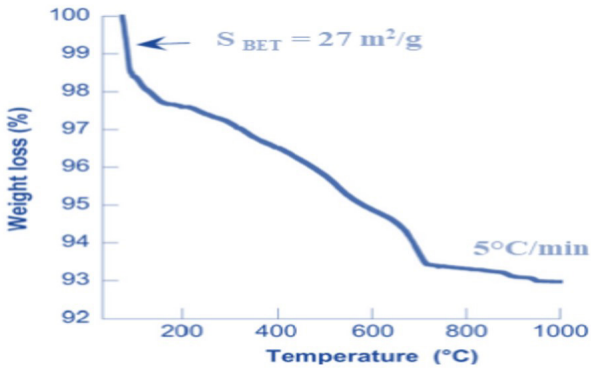

Figure 3: BET and TGA analysis of the raw oil shale.

Optimization of the adsorption process

The final equation by coded factors

The true factors equation was used to make predictions on specific levels of each factor. The coded mathematical model of the 15-factors design can be represented as:

$$R\ (mg/g) = X_0 + X_1 * \text{Mass} + X_2 * \text{Initial concentration} - X_3 * \text{Contact Time} - X_4 * \text{Mass} * \text{Initial concentration} + X_5 * \text{Mass} * C + X_6 * \text{Initial concentration} * \text{Contact Time} - X_7 * \text{Mass}^2 - X_8 * \text{Initial concentration}^2 - X_9 * \text{Contact Time}^2$$

By replacing the values of the regression coefficients (X_i) in the equation, we obtain R (%), which indicates the percentage removal of CIP. X_0 refers to the global mean. Then we get:

$$R\ (mg/g) = 3.44441 + 25{,}0753 * A + 0.211381 * B - 0.0127731 * C - 0.605614 * A * B + 0.222206 * A * C + 0.000596343 * B * C - 39.1306 * A^2 - 0.000233504 * B^2 - 7.81347e\text{-}05 * C^2$$

A coded equation is useful for identifying the relative influence of factors by comparing factor coefficients.

Analysis of variance (ANOVA)

Once the main effects were estimated, an ANOVA (Table 4) was performed to determine interaction factors affecting ciprofloxacin elimination.

The column labeled "df" gives the degrees of freedom for each source. In the response surface methodology, the degrees of freedom are the same number of model coefficients added sequentially row by row.

The F value of the Subplot of 19.99 implies that the model is significant. There is only a 0.2% chance that such a high F value is due to noise.

Table 4: ANOVA results.

Source	Term df	Error df	F-value	p-value	
Subplot	7	5.00	19.99	0.0023	**Significant**
B-B	1	5.00	36.00	0.0018	
C-C	1	5.00	63.41	0.0005	
AB	1	5.00	6.93	0.0464	
AC	1	5.00	14.79	0.0120	
BC	1	5.00	13.59	0.0142	
B^2	1	5.00	0.0669	0.8062	
C^2	1	5.00	1.99	0.2175	

p-values below 0.0500 indicate that the model terms are significant [30]. In this case, B, C, AB, AC, and BC are significant model terms. Values above 0.1000 indicate that the model terms are not significant. If the model has many irrelevant terms (Disregarding the terms needed to support the hierarchy), the model reduction can improve your model [31].

Fit statistics

To model the statistics, the standard deviation, overall mean of all response data (Mean), Adj R-squared, coefficient of variation (C.V), and R-squared, must be calculated. The results of the previous parameters are presented in table 5.

Table 5: Modeling statistics.

Std. Dev.	3.13	**R^2**	0.9668
Mean	19.44	**Adjusted R^2**	0.8448
C.V. %	16.12		

The R^2 of 0.9668 is in reasonable agreement with the Adjusted R^2 of 0.8448; the difference indicates that this model can be used to navigate the design space.

Figure 4 shows the optimized response of different parameters used in the adsorption process [32], initial CIP concentration, contact time, and OST100 mass. The removal efficiency (21.194 mg/g) was obtained with an initial CIP concentration value of 21.838 mg/L; contact time of 270.289 min; and a mass of OST100 of 0.317 g.

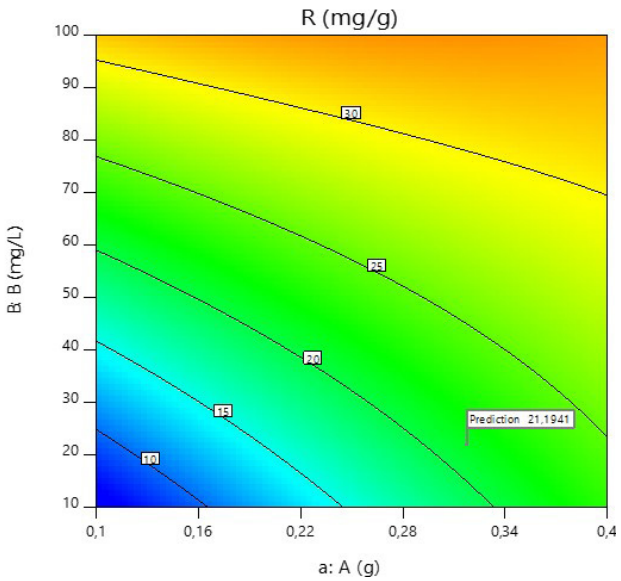

Figure 4: Optimized response.

Conclusion

Data from this study showed that steamed oil shales have been used successfully for the removal of organic species CIP. To enhance efficiency, a two-level full factorial design was implemented using Design-Expert 11 software, eliminating the need for traditional one-factor experiments and reducing the number of trials while optimizing time. ANOVA was utilized to determine the key process variables that influenced CIP adsorption efficiency. By employing a full factorial design with two levels (2^k), the most significant parameters were identified within the tested conditions. The primary factors, including the initial concentration of ciprofloxacin, contact time, and mass of raw oil shales, exhibited substantial effects. Similarly, the removal efficiency (21.194 mg/g) was obtained with an initial CIP concentration value of 21.838 mg/L; contact time of 270.289 min; and a mass of OST100 of 0.317 g. Furthermore, considering the experimental results it can be concluded that the examined adsorbent material holds great potential for effectively treating wastewater and industrial effluents for pollution mitigation purposes.

Acknowledgements

The authors would like to thank the Mohamed V University of Rabat, Morocco, for the financial support of this work.

Conflict of Interest

The authors declare no conflict of interest.

Funding

This study received no external funding.

References

1. Singh R, Singh AP, Kumar S, Giri BS, Kim KH. 2019. Antibiotic resistance in major rivers in the world: a systematic review on occurrence, emergence, and management strategies. *J Clean Prod* 234: 1484-1505. https://doi.org/10.1016/j.jclepro.2019.06.243
2. Arif A, Malik MF, Liaqat S, Aslam A, Mumtaz K, et al. 2020. Water pollution and industries. *Pure Appl Biol* 9(4): 2214-2224. http://dx.doi.org/10.19045/bspab.2020.90237
3. Iordache AM, Nechita C, Pluhacek T, Iordache M, Zgavarogea R, et al. 2020. Past and present anthropic environmental stress reflect high susceptibility of natural freshwater ecosystems in Romania. *Environ Pollut* 267: 115505. https://doi.org/10.1016/j.envpol.2020.115505
4. Aniagor CO, Menkiti MC. 2018. Kinetics and mechanistic description of adsorptive uptake of crystal violet dye by lignified elephant grass complexed isolate. *J Environ Chem Eng* 6(2): 2105-2118. https://doi.org/10.1016/j.jece.2018.01.070
5. Al-Ghouti MA, Al-Kaabi MA, Ashfaq MY, Da'na DA. 2019. Produced water characteristics, treatment and reuse: a review. *J Water Process Eng* 28: 222-239. https://doi.org/10.1016/j.jwpe.2019.02.001

6. Tran NH, Reinhard M, Gin KYH. 2018. Occurrence and fate of emerging contaminants in municipal wastewater treatment plants from different geographical regions-a review. *Water Res* 133: 182-207. https://doi.org/10.1016/j.watres.2017.12.029
7. Ruiz-Hitzky E, Aranda P, Akkari M, Khaorapapong N, Ogawa M. 2019. Photoactive nanoarchitectures based on clays incorporating TiO_2 and ZnO nanoparticles. *Beilstein J Nanotechnol* 10(1): 1140-1156. https://doi.org/10.3762/bjnano.10.114
8. Igwegbe CA, Oba SN, Aniagor CO, Adeniyi AG, Ighalo JO. 2021. Adsorption of ciprofloxacin from water: a comprehensive review. *J Ind Eng Chem* 93: 57-77. https://doi.org/10.1016/j.jiec.2020.09.023
9. Chen J, Tong T, Jiang X, Xie S. 2020. Biodegradation of sulfonamides in both oxic and anoxic zones of vertical flow constructed wetland and the potential degraders. *Environ Pollut* 265: 115040. https://doi.org/10.1016/j.envpol.2020.115040
10. Hong X, Zhao Y, Zhuang R, Liu J, Guo G, et al. 2020. Bioremediation of tetracycline antibiotics-contaminated soil by bioaugmentation. *RSC Adv* 10(55): 33086-33102. https://doi.org/10.1039/d0ra04705h
11. Yang Y, Ok YS, Kim KH, Kwon EE, Tsang YF. 2017. Occurrences and removal of pharmaceuticals and personal care products (PPCPs) in drinking water and water/sewage treatment plants: a review. *Sci Total Environ* 596: 303-320. https://doi.org/10.1016/j.scitotenv.2017.04.102
12. Qiao M, Ying GG, Singer AC, Zhu YG. 2018. Review of antibiotic resistance in China and its environment. *Environ Int* 110: 160-172. https://doi.org/10.1016/j.envint.2017.10.016
13. Patel M, Kumar R, Kishor K, Mlsna T, Pittman CU, et al. 2019. Pharmaceuticals of emerging concern in aquatic systems: chemistry, occurrence, effects, and removal methods. *Chem Rev* 119(6): 3510-3673. https://doi.org/10.1021/acs.chemrev.8b00299
14. Yang Z, Zhou Y, Feng Z, Rui X, Zhang T, et al. 2019. A review on reverse osmosis and nanofiltration membranes for water purification. *Polymers* 11(8): 1252. https://doi.org/10.3390/polym11081252
15. Mohammed AA, Selman HM. 2018. Liquid surfactant membrane for lead separation from aqueous solution: studies on emulsion stability and extraction efficiency. *J Environ Chem Eng* 6(6): 6923-6930. https://doi.org/10.1016/j.jece.2018.10.021
16. Chen Q, Yao Y, Li X, Lu J, Zhou J, et al. 2018. Comparison of heavy metal removals from aqueous solutions by chemical precipitation and characteristics of precipitates. *J Water Process Eng* 26: 289-300. https://doi.org/10.1016/j.jwpe.2018.11.003
17. Rajesh AM, Bhatt SA, Brahmbhatt H, Anand PS, Popat KM. 2015. Taste masking of ciprofloxacin by ion-exchange resin and sustain release at gastric-intestinal through interpenetrating polymer network. *Asian J Pharm Sci* 10(4): 331-340. https://doi.org/10.1016/j.ajps.2015.01.002
18. Alonso JJS, El Kori N, Melián-Martel N, Del Río-Gamero B. 2018. Removal of ciprofloxacin from seawater by reverse osmosis. *J Environ Manag* 217: 337-345. https://doi.org/10.1016/j.jenvman.2018.03.108
19. Habiba U, Mutahir S, Khan MA, Humayun M, Refat MS, et al. 2022. Effective removal of refractory pollutants through cinnamic acid-modified wheat husk biochar: experimental and DFT-based analysis. *Catalysts* 12(9): 1063. https://doi.org/10.3390/catal12091063
20. Banerjee S, Jana A, Mukherjee D, Ghosh S, Chakrabarti S, et al. 2019. Synthesis of Hydrophobic Ceramic Ultrafiltration Membrane and Performance Evaluation for Removal of Ciprofloxacin in Water. In Ghosh S (eds) Waste Water Recycling and Management. Springer, Singapore, pp 65-73.
21. Mondal SK, Saha AK, Sinha A. 2018. Removal of ciprofloxacin using modified advanced oxidation processes: kinetics, pathways and process optimization. *J Clean Prod* 171: 1203-1214. https://doi.org/10.1016/j.jclepro.2017.10.091
22. Zheng C, Zheng H, Hu C, Wang Y, Wang Y, et al. 2020. Structural design of magnetic biosorbents for the removal of ciprofloxacin from water. *Bioresour Technol* 296: 122288. https://doi.org/10.1016/j.biortech.2019.122288
23. Sayyed AJ, Pinjari DV, Sonawane SH, Bhanvase BA, Sheikh J, et al. 2021. Cellulose-based nanomaterials for water and wastewater treatments: a review. *J Environ Chem Eng* 9(6): 106626. https://doi.org/10.1016/j.jece.2021.106626
24. Loukilia H, Mabroukic J, Anouzlab A, Kouzia Y, Younssia SA, et al. 2021. Pre-treated Moroccan natural clays: application to the wastewater treatment of textile industry. *Desalin Water Treat* 240: 124-136. https://doi.org/10.5004/dwt.2021.27644
25. Saoiabi S, Latifi S, Gouza A, El Hammari L, Boukra O, et al. 2022. Elimination of heavy metal Ni^{2+} from wastewater using Moroccan oil shale as bio sorbent. *Mater Today Proc* 58: 987-993. https://doi.org/10.1016/j.matpr.2021.12.457
26. Abrouki Y, Mabrouki J, Anouzla A, Rifi SK, Zahiri Y, et al. 2021. Optimization and modeling of a fixed-bed biosorption of textile dye using agricultural biomass from the Moroccan Sahara. *Desalin Water Treat* 240: 144-151. https://doi.org/10.5004/dwt.2021.27704
27. Anouzla A, Kastali M, Azoulay K, Bencheikh I, Fattah G, et al. 2022. Multi-response optimization of coagulation–flocculation process for stabilized landfill leachate treatment using a coagulant based on an industrial effluent. *Desalin Water Treat* 254: 71-79. https://doi.org/10.5004/dwt.2022.28388
28. Gouza A, Saoiabi S, El Karbane M, Masse S, Laurent G, et al. 2017. Oil shale powders and their interactions with ciprofloxacin, ofloxacin, and oxytetracycline antibiotics. *Environ Sci Pollut Res* 24: 25977-25985. https://doi.org/10.1007/s11356-017-0100-5
29. Chafyq EH, Legrouri K, Oumam M, Mansouri S, Aghrouch M, et al. 2021. Optimization of operational conditions using the experimental design method to remove *Escherichia coli* from contaminated groundwater by an adsorbent material prepared from Moroccan oil shales. *Groundw Sustain Dev* 12: 100532. https://doi.org/10.1016/j.gsd.2020.100532
30. Zhang W, Wang D, Sun Z, Song J, Deng X. 2021. Robust superhydrophobicity: mechanisms and strategies. *Chem Soc Rev* 50(6): 4031-4061. https://doi.org/10.1039/d0cs00751j
31. Majd MM, Kordzadeh-Kermani V, Ghalandari V, Askari A, Sillanpää M. 2022. Adsorption isotherm models: a comprehensive and systematic review (2010-2020). *Sci Total Environ* 812: 151334. https://doi.org/10.1016/j.scitotenv.2021.151334
32. Stevens NT, Hagar L. 2022. Comparative probability metrics: using posterior probabilities to account for practical equivalence in A/B tests. *Am Stat* 76(3): 224-237. https://doi.org/10.1080/00031305.2021.2000495